RSC Advances

PAPER

View Article Online
View Journal | View Issue

Cite this: *RSC Adv.*, 2017, **7**, 20795

An amino-coordination metal–organic framework for highly selective C_2H_2/CH_4 and C_2H_2/C_2H_4 separations through the appropriate control of window sizes†

Ling Zhang,[a] Xili Cui,[b] Huabin Xing,[b] Yu Yang,[a] Yuanjing Cui,[a] Banglin Chen*[ac] and Guodong Qian*[a]

Received 6th March 2017
Accepted 30th March 2017

DOI: 10.1039/c7ra02741a

rsc.li/rsc-advances

The efficient separation of C_2H_2 *versus* C_2H_4 and CH_4 to obtain high-purity C_2H_2 and C_2H_4 is of significance for making full, economic use of these raw chemicals. Herein, an amino-coordination microporous metal–organic framework **ZJU-198**, ZnL·DMF (ZJU = Zhejiang University, L = (2*E*,2*E*′)-3,3′-(5-amino-1,3-phenylene)diacrylic acid, DMF = *N*,*N*′-dimethylformamide), has been demonstrated as a valuable adsorbent for C_2H_2/C_2H_4 and C_2H_2/CH_4 separations. The activated **ZJU-198a** exhibits moderate C_2H_2 uptakes (99.4 cm^3 cm^{-3} for 273 K and 98.4 cm^3 cm^{-3} for 298 K under 1.0 bar) and moderately high C_2H_2/C_2H_4 selectivity (5.8 to 7.7 at 273 K and 4.8 to 7.2 at 298 K). Specifically, the C_2H_2/CH_4 selectivity of **ZJU-198a** reaches up to 497.9 and 391.1 at 273 K and 298 K, respectively. To the best of our knowledge, the C_2H_2/CH_4 selectivity coefficients of **ZJU-198a** at both 298 K and 273 K are the highest values among the reported metal–organic frameworks, meaning that there is bright potential for **ZJU-198a** in hydrocarbon storage and separation.

Introduction

C_2 hydrocarbons are generally recognized as important raw chemicals to the petrochemical industries.[1] The efficient separation of C_2H_2/C_2H_4 can make full, economic use of these raw chemicals. Ethylene is mainly produced from steam cracking of an alkane. However, the presence of spin-off acetylene has an impeditive effect on further polymerization of ethylene. That is why the C_2H_2 purity of the C_2H_2/C_2H_4 mixture must be guaranteed below 40 ppm.[2–4] What's more, acetylene that is chiefly yielded by the cracking of petroleum generally contains the adverse by-product methane (CH_4).[5] Therefore, the efficient separation of C_2H_2 over C_2H_4 and CH_4 to obtain high-purity C_2H_4 and C_2H_2 is of economic significance.

Porous materials might offer alternative approaches over energy-consumptive commercial materials. Extensive efforts have been engaged in hydrocarbon adsorption and separation. During the past decades, microporous metal–organic frameworks (MOFs) have attracted substantial attention in gas storage and separation.[6–15] Compared with other porous adsorbents, such as activated carbons and molecular sieves, MOFs have greater potential both at a research and application level by virtue of their attractive advantages.[16–35] On the one hand, the high porosity of MOFs allows them to take up large amounts of gas molecules; on the other hand, the easily-adjustable pore/window sizes and functionalization within MOFs offer significant improvements in gas separation selectivity.[36–40]

In terms of gas separation, the pores within MOFs can be judiciously modified through the immobilization of specific sites like Lewis basic sites (LBSs) and functional groups including amino groups to enhance the interaction between the framework and preferred gas molecules.[41–43] However, the aforementioned strategies bring a costly regeneration bill. This worrisome issue can be addressed through the accurate control of the pore/window sizes. Herein, our previously reported amino-coordination microporous metal–organic framework **ZJU-198**, which was validated as one of the best performing metal–organic frameworks for CO_2/N_2 separation,[44] has been chosen with the appropriate window sizes and synthesized successfully. The activated **ZJU-198a** has been further demonstrated as a valuable adsorbent for C_2H_2/C_2H_4 and C_2H_2/CH_4 separations and exhibited moderate C_2H_2 storages (99.4 cm^3 cm^{-3} at 273 K and 98.4 cm^3 cm^{-3} at 298 K under 1.0 bar) and

[a]*State Key Laboratory of Silicon Materials, Cyrus Tang Center for Sensor Materials and Applications, Department of Materials Science & Engineering, Zhejiang University, Hangzhou 310027, China. E-mail: gdqian@zju.edu.cn*

[b]*College of Chemical and Biological Engineering, Zhejiang University, Hangzhou 310027, China*

[c]*Department of Chemistry, University of Texas at San Antonio, One UTSA Circle, San Antonio, Texas 78249-0698, USA. E-mail: banglin.chen@utsa.edu; Fax: +1-210-458-7428*

† Electronic supplementary information (ESI) available: syntheses; TGA; IR; XRD; breakthrough test. See DOI: 10.1039/c7ra02741a

moderately high C_2H_2/C_2H_4 selectivity (5.8 to 7.7 at 273 K and 4.8 to 7.2 at 298 K). It's worth noting that **ZJU-198a** has been further demonstrated for C_2H_2/CH_4 separation with very high selectivity of 63.1 to 497.9 and 69.0 to 391.1 at 273 K and 298 K, respectively. To the best of our knowledge, **ZJU-198a** exhibits the highest performance for the separation of C_2H_2/CH_4 both at 298 K and 273 K among the reported metal–organic frameworks, meaning that there is bright potential for **ZJU-198a** in hydrocarbon storage and separations.

Experimental

Materials and methods

All solvents and reagents except the organic ligand were commercially available and used without further purification. The syntheses of the organic linker (2*E*,2*E*′)-3,3′-(5-amino-1,3-phenylene)diacrylic acid, simplified as 5-amino-H_2L, and **ZJU-198** are referred to in our previously reported work.[44] ^{1}H NMR spectra were obtained using a Bruker Advance DMX 500 MHz spectrometer with tetramethylsilane (TMS) as an internal standard. Elemental analyses (EA) for C, H, and N were performed using an EA1112 microelemental analyzer. Infrared spectra (IR) were obtained using a Thermo Fisher Nicolet iS10 spectrometer using KBr pellets. Thermogravimetric analyses (TGA) were performed using a Netzsch TG209F3 with a heating rate of 10 °C min^{-1} under the protection of a high-purity N_2 atmosphere. All gas sorption isotherms were obtained using a Micromeritics ASAP 2020 surface area analyzer. The activation procedure of **ZJU-198** also corresponded to our previously reported work.[44] The sorption measurements were maintained at 196 K with a mixture of drikold and acetone. Ice-water and water baths were used for the adsorption isotherms of C_2H_2, C_2H_4 and CH_4 at 273 K and 298 K, respectively.

Ideal adsorbed solution theory (IAST)

The selectivity of the preferential adsorption of component 1 over component 2 in a mixture containing 1 and 2 can be formally defined as:

$$S_{ads} = \frac{q_1/q_2}{p_1/p_2}$$

In the above equation, q_1 and q_2 are the absolute component loadings of the adsorbed phase in the mixture. These component loadings are also termed the uptake capacity. We calculated the values of q_1 and q_2 using the Ideal Adsorbed Solution Theory (IAST) of Myers and Prausnitz.

The isosteric heat, Q_{st}

The isosteric heat of C_2H_2, C_2H_4, and CH_4 adsorption, Q_{st}, defined as

$$Q_{st} = RT^2 \left(\frac{\partial \ln P}{\partial T}\right)$$

was determined using the Clausius–Clapeyron equation by fitting the adsorption isotherms taken at 273 K and 298 K to a Langmuir expression.

Results and discussion

The solvothermal reaction of the organic ligand 5-amino-H_2L with $Zn(NO_3)_2 \cdot 6H_2O$ in a mixture of solvents DMF/H_2O/acetonitrile afforded **ZJU-198** as colorless layer-shaped crystals, which has a formula of ZnL·DMF (DMF = *N*,*N*-dimethylformamide) determined by single-crystal X-ray diffraction and elemental analysis (EA). The purity of the phase was further indicated by powder X-ray diffraction (PXRD).

Single-crystal X-ray diffraction analysis demonstrates that **ZJU-198** crystallizes in the space group of *Pbca* with a (4, 5)-coordination network. It's clear to see that each Zn1 atom exhibits 5-coordination connecting with O1A, O3, O13, O18, and N9 from four different organic linkers to construct an asymmetric pentahedron as the secondary building unit (SBU) (Fig. 1b). Furthermore, the four oxygen atoms and the nitrogen atom of the same organic linker coordinate to four different Zn1 atoms (Fig. 1a). The O1A atom and O3 atom from the same bidentate carboxylate group connect two different Zn1 atoms while O13 and O18 exhibit the same coordination condition. The SBUs link the organic ligands further to form a three-dimensional (3D) framework. It's worth noting that the zigzag coordination tendency makes the unique orderly overlapping channels, but with no interpenetration of the framework (Fig. 1d–f). Only two types of channel exist, which are approximately 3.6 Å × 4.1 Å and 2.1 Å × 5.0 Å as viewed from the *a* axis (Fig. 1c), and the van der Waals radii of the atoms have been already been taken into account when labelling the size of these channels.

After sufficient acetone-exchange and suitable activation, the CO_2 sorption at 196 K is further operated to explore the porosity of desolvated **ZJU-198a**. As depicted in Fig. S5,† the sorption data of CO_2-196 K is consistent with the typical type-I sorption characteristic with a Langmuir surface area and BET of 488.5 m^2 g^{-1} and 343.1 m^2 g^{-1}, respectively. As for the applicable window size and moderate porosity of **ZJU-198a**, we were encouraged to explore the adsorption performance of C_2H_2, C_2H_4, and CH_4 at low pressures. Herein, the low-pressure adsorption isotherms of C_2H_2, C_2H_4, and CH_4 at 273 K and 298 K are illustrated in Fig. 2. Compared with C_2H_4 and CH_4, it's exciting that the C_2H_2 adsorption capacity of **ZJU-198a** zooms up rapidly to reach saturation even at extremely low pressure. Under 0.01 bar, **ZJU-198a** takes up a great amount of 72.5 cm^3 cm^{-3}, 37.3 cm^3 cm^{-3}, and 0.13 cm^3 cm^{-3} for C_2H_2, C_2H_4, and CH_4 at 273 K, respectively and 41.4 cm^3 cm^{-3}, 3.1 cm^3 cm^{-3}, and 0.03 cm^3 cm^{-3} for C_2H_2, C_2H_4, and CH_4 at 298 K, respectively. The saturation capacities of C_2H_2, C_2H_4, and CH_4 are 99.4 cm^3 cm^{-3}, 92.4 cm^3 cm^{-3}, and 21.1 cm^3 cm^{-3} at 273 K, respectively, and 98.4 cm^3 cm^{-3}, 89.2 cm^3 cm^{-3}, and 8.8 cm^3 cm^{-3} at 298 K, respectively. It's worth noting that there is almost no decline in C_2H_2 adsorption with the temperature rise, and the CH_4 molecule has no competitive advantages against the C_2H_2 molecule especially at extremely low pressure.

The adsorption selectivity for C_2H_2 over C_2H_4 and CH_4 is another prerequisite for assessing an adsorbent material, except for when assessing the mono-component adsorption. As

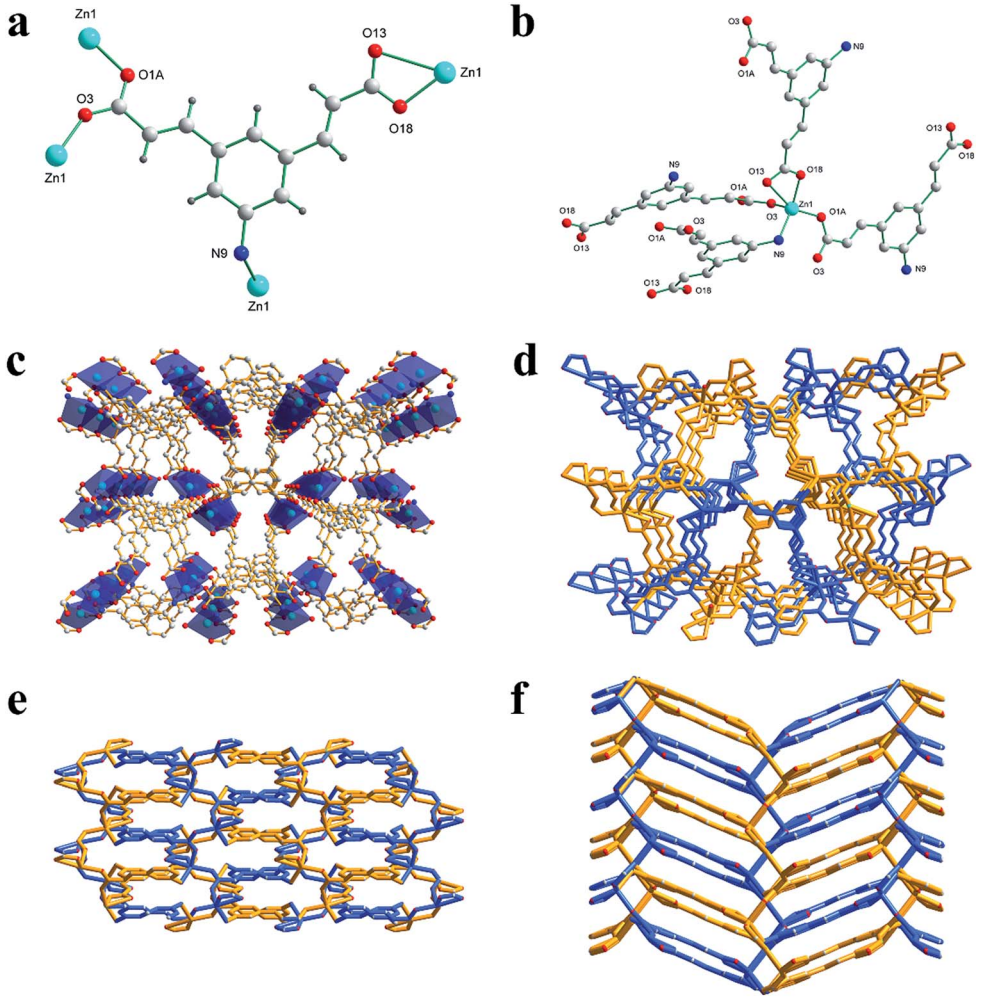

Fig. 1 The X-ray single crystal structure of **ZJU-198**, indicating that (a) the organic ligand 5-amino-H_2L coordinates four Zn^{2+}; (b) each Zn^{2+} exhibits 5-coordination that connects four different organic linkers to construct an asymmetric pentahedron at the secondary building site (SBU); (c) the zigzag channels of about 3.6 Å × 4.1 Å and 2.1 Å × 5.0 Å are viewed from the *a* axis; (d–f) the coordination tendency of the orderly overlapping framework (C, gray; O, red; Zn, cyan; N, blue; H atoms are omitted for clarity).

is well-known, the Ideal Adsorbed Solution Theory (IAST) is recognized to estimate the gas adsorption separation. Thus, the results of the IAST calculation for C_2H_2/C_2H_4 (1 : 99, v/v) and C_2H_2/CH_4 (50 : 50, v/v) are expressed in Fig. 3. The selectivity coefficients of C_2H_2/C_2H_4 are 5.8 to 7.7 at 273 K and 4.8 to 7.2 at 298 K, respectively. It's quite surprising to read that the selectivity of C_2H_2/CH_4 reaches up to 497.9 and 391.1 for 273 K and 298 K, respectively. Table 1 lists the comparison of **ZJU-198a** with some other promising MOFs for C_2H_2/CH_4 separation.[45–50] We are compelled to admit that the C_2H_2 adsorption capacity of **ZJU-198a** is moderately limited by the relatively low porosity. However, the C_2H_2/CH_4 selectivity of **ZJU-198a** drastically outperforms those of other MOFs. To the best of our knowledge, the C_2H_2/CH_4 selectivity coefficients of **ZJU-198a** at both 273 K and 298 K are the highest values among the as yet reported metal–organic frameworks (MOFs).

The moderate gas capacity and excellent gas separation make **ZJU-198a** a valuable candidate for hydrocarbon adsorption and separation. Furthermore, the regeneration energy cost attributed to the binding energy is another essential consideration. The binding energy between the adsorbed gas molecule and framework is reflected in the isosteric heat of adsorption (Q_{st}). Fig. 4 illustrates the isosteric heat of C_2H_2, C_2H_4, and CH_4 with **ZJU-198a**. Unexpectedly, the isosteric heat of C_2H_4 (37.4 kJ mol^{-1}) is higher than that of C_2H_2 (26.1 kJ mol^{-1}), C_2H_4, and CH_4 (16.2 kJ mol^{-1}).

The discrepancy between the C_2H_2 molecule and C_2H_4 molecule is distinctly far less than that between the C_2H_2 molecule and CH_4 molecule. This is a reasonable excuse for the performance of the C_2H_2/C_2H_4 separation of **ZJU-198a** not looking as outstanding as that of C_2H_2/CH_4. However, there is still a hysteretic circumstance about the adsorption of C_2H_4 *versus* C_2H_2 especially at the extremely-low pressure referred to in the insets of Fig. 2. Herein, transient breakthrough simulations were carried out to separate the feed gases C_2H_2/C_2H_4 (1 : 99, v/v), the typical industrial ingredient. As is shown in Fig. 5, the C_2H_2/C_2H_4 mixture is clearly separated by **ZJU-198a**. After a certain time (τ_{break}, 64.5 minutes), the impurity level of

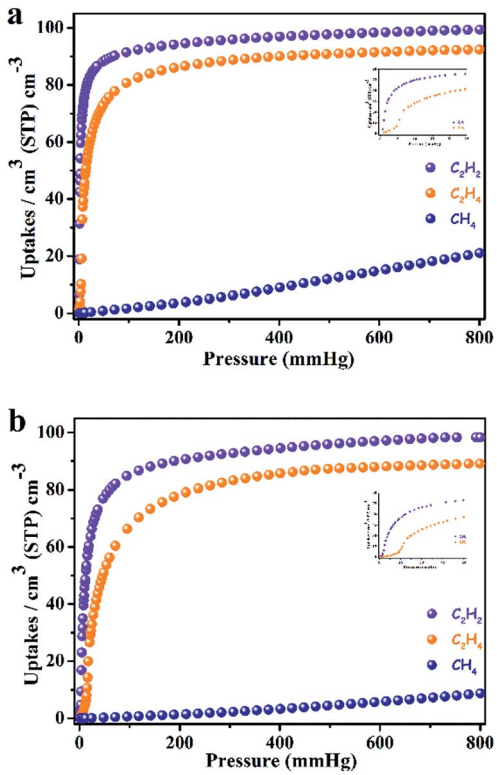

Fig. 2 The single-component adsorption isotherms for C_2H_2 (violet), C_2H_4 (orange), and CH_4 (blue) of **ZJU-198a** at 273 K (a) and 298 K (b). The insets exhibit the adsorption data of C_2H_2 and C_2H_4 at extremely low pressure.

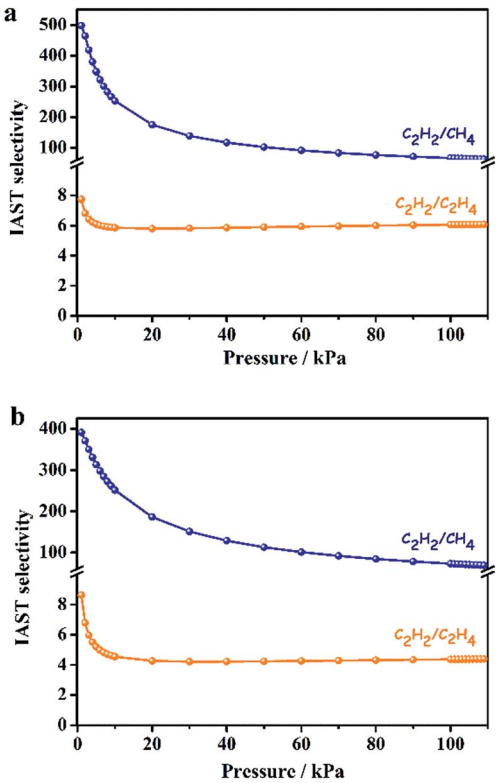

Fig. 3 (a) The IAST calculations of C_2H_2/C_2H_4 and C_2H_2/CH_4 adsorption selectivity for **ZJU-198a** at 273 K; (b) the IAST calculations of C_2H_2/C_2H_4 and C_2H_2/CH_4 adsorption selectivity for **ZJU-198a** at 298 K.

C_2H_2 exceeded the purity level at 40 ppm. During the time $0 \sim \tau_{break}$, the amount of C_2H_2 captured in **ZJU-198a** is 126.8 mmol L^{-1}, which is still a satisfactory value.

The crystal structure analysis was carried out to demonstrate the excellent C_2H_2/CH_4 and C_2H_2/C_2H_4 separations of **ZJU-198a**. Note that the empirical kinetic sizes of C_2H_2, C_2H_4, and CH_4 are 3.32 Å × 3.34 Å, 3.28 Å × 4.18 Å, and 3.82 Å × 3.94 Å, respectively.[51] It's clear to see that there only exists one available window of **ZJU-198a** of approximately 3.6 Å × 4.1 Å, which is slightly larger than the size of the C_2H_2 molecule, close to that of the C_2H_4 molecule while smaller than that of the CH_4 molecule. Herein, it's easy to understand that the good-enough window of the framework plays an important role in selecting the preferential C_2H_2 molecule and closing the door on the CH_4 molecule. How does the relatively low porosity of **ZJU-198a** feature in the moderately high C_2H_2 adsorption? The C_2H_2 molecules were captured in the framework and the diffusion between the adjacent channels was limited by the narrow channels. Therefore, **ZJU-198a** with orderly overlapping channels exhibits moderately high C_2H_2 storage and excellent C_2H_2/CH_4 and C_2H_2/C_2H_4 separations.

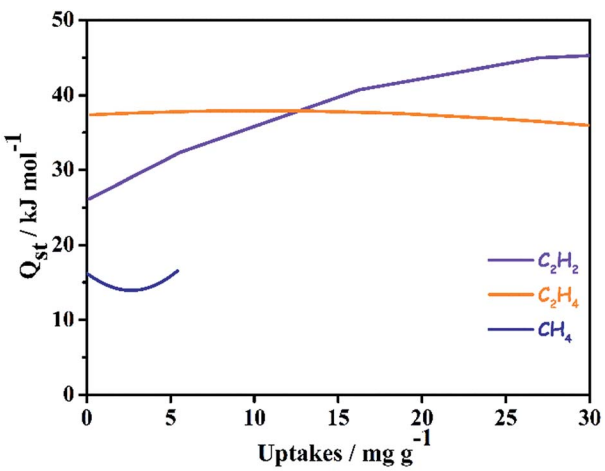

Fig. 4 The isosteric heat of C_2H_2, C_2H_4, and CH_4 adsorption, Q_{st}, in ZJU-198a.

Conclusions

The amino-coordination microporous metal–organic framework **ZJU-198** with a good-enough window has been synthesized successfully and further demonstrated as a valuable adsorbent. The activated **ZJU-198a** exhibits moderate C_2H_2 storage and excellent C_2H_2/CH_4 and C_2H_2/C_2H_4 separations. Especially, the selectivity of C_2H_2/CH_4 is the highest value among the as yet reported metal–organic frameworks (MOFs). Herein, we believe that making the best of the size-sieving effect of the framework

Table 1 The comparison of the adsorption data for selected MOFs

MOFs	Surface area (m^2 g^{-1}, BET)	C_2H_2 uptake (at 1.0 bar, RT, cm^3 g^{-1})	Selectivity for C_2H_2/CH_4	Q_{st} of C_2H_2 (kJ $mmol^{-1}$)	Ref.
ZJNU-55	450	56.3	64.9	42.4	46
BUT-70A	695	69.5	66.6	25.6	47
UTSA-5a	462	59.8	28.4	30.8	48
Cu-TDPAH	—	177.7	127.1	42.5	45
UTSA-50a	604	90.6	68	39.4	50
ZJU-199a	987	128.0	33.5	38.5	49
ZJU-198a	**343**	**72.9**	**391.1**	**26.1**	**This work**

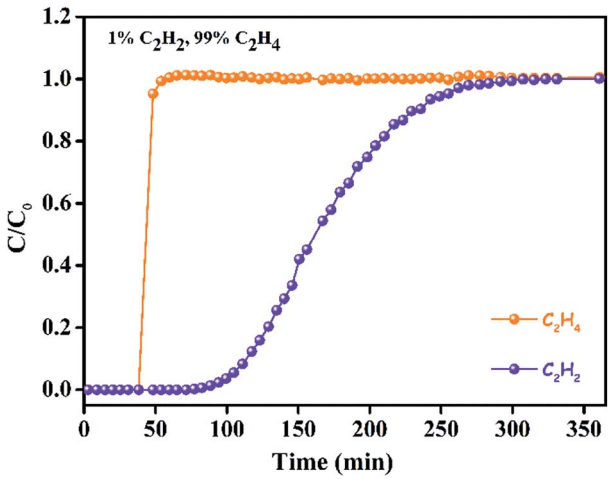

Fig. 5 The breakthrough curves of **ZJU-198a** for the C_2H_2/C_2H_4 separation (1 : 99; v/v) operated at 1 bar and 298 K. C_A and C_0 are the concentrations of each gas at the inlet and outlet, respectively.

to achieve efficient gas separation will be a significant approach for further applications.

Acknowledgements

This work was supported by the National Natural Science Foundation of China (No. 51472217 and 51432001), the Zhejiang Provincial Natural Science Foundation of China (No. LR13E020001 and LZ15E020001), and the Fundamental Research Funds for the Central Universities (No. 2015QNA4009 and 2016FZA4007), and it was partly supported by the Welch Foundation (AX-1730).

Notes and references

1 R. Krishna, *RSC Adv.*, 2015, **5**, 52269.
2 X. L. Cui, K. J. Chen, H. B. Xing, Q. W. Yang, R. Krishna, Z. B. Bao, H. Wu, W. Zhou, X. L. Dong, Y. Han, B. Li, Q. L. Ren, M. J. Zaworotko and B. L. Chen, *Science*, 2016, **353**, 141.
3 T.-L. Hu, H. L. Wang, B. Li, R. Krishna, H. Wu, W. Zhou, Y. F. Zhao, Y. Han, X. Wang, W. D. Zhu, Z. Z. Yao, S. C. Xiang and B. L. Chen, *Nat. Commun.*, 2015, **6**, 7328.
4 H.-M. Wen, H. Wang, B. Li, Y. Cui, H. Wang, G. Qian and B. Chen, *Inorg. Chem.*, 2016, **55**, 7214.
5 Y.-X. Tan, Y.-P. He and J. Zhang, *RSC Adv.*, 2015, **5**, 7794.
6 W. G. Lu, Z. W. Wei, Z.-Y. Gu, T.-F. Liu, J. Park, J. Park, J. Tian, M. W. Zhang, Q. Zhang, T. Gentle, M. Bosch and H.-C. Zhou, *Chem. Soc. Rev.*, 2014, **43**, 5561.
7 Y. Bai, Y. B. Dou, L.-H. Xie, W. Rutledge, J.-R. Li and H.-C. Zhou, *Chem. Soc. Rev.*, 2016, **45**, 2327.
8 H. Wang, J. Xu, D.-S. Zhang, Q. Chen, R.-M. Wen, Z. Chang and X.-H. Bu, *Angew. Chem., Int. Ed.*, 2015, **54**, 5966.
9 Z. Chang, D.-H. Yang, J. Xu, T.-L. Hu and X.-H. Bu, *Adv. Mater.*, 2015, **27**, 5432.
10 Y. Fang, W. Liu, S. J. Teat, G. Dey, Z. Shen, L. An, D. Yu, L. Wang, D. M. O'Carroll and J. Li, *Adv. Funct. Mater.*, 2017, **27**, 1603444.
11 K. Sasan, Q. P. Lin, C. Y. Mao and P. Y. Feng, *Nanoscale*, 2016, **8**, 10913.
12 K. Liu, B. Li, Y. Li, X. Li, F. Yang, G. Zeng, Y. Peng, Z. Zhang, G. Li, Z. Shi, S. Feng and D. Song, *Chem. Commun.*, 2014, **50**, 5031.
13 Y. He, R. Krishna and B. Chen, *Energy Environ. Sci.*, 2012, **5**, 9107.
14 K. Jiang, L. Zhang, Q. Hu, D. Zhao, T. Xia, W. Lin, Y. Yang, Y. Cui, Y. Yang and G. Qian, *J. Mater. Chem. B*, 2016, **4**, 6398.
15 D.-M. Chen, J.-Y. Tian, C.-S. Liu and M. Du, *CrystEngComm*, 2016, **18**, 3760.
16 D. Zhao, D. Yue, K. Jiang, Y. Cui, Q. Zhang, Y. Yang and G. Qian, *J. Mater. Chem. C*, 2017, **5**, 1607.
17 Y.-N. Gong, T. Ouyang, C.-T. He and T.-B. Lu, *Chem. Sci.*, 2016, **7**, 1070.
18 M. Zhang, Y.-L. Huang, J.-W. Wang and T.-B. Lu, *J. Mater. Chem. A*, 2016, **4**, 1819.
19 M.-Y. Gao, F. Wang, Z.-G. Gu, D.-X. Zhang, L. Zhang and J. Zhang, *J. Am. Chem. Soc.*, 2016, **138**, 2556.
20 B. Li, H.-M. Wen, Y. Cui, W. Zhou, G. Qian and B. Chen, *Adv. Mater.*, 2016, **28**, 8819.
21 J. Cai, H. Wang, H. Wang, X. Duan, Z. Wang, Y. Cui, Y. Yang, B. Chen and G. Qian, *RSC Adv.*, 2015, **5**, 77417.
22 J.-W. Zhang, M.-C. Hu, S.-N. Li, Y.-C. Jiang and Q.-G. Zhai, *Dalton Trans.*, 2017, **46**, 836.
23 W.-Y. Gao, C.-Y. Tsai, L. Wojtas, T. Thiounn, C.-C. Lin and S. Ma, *Inorg. Chem.*, 2016, **55**, 7291.
24 Q. Sun, B. Aguila, J. Perman, N. Nguyen and S. Ma, *J. Am. Chem. Soc.*, 2016, **138**, 15790.

25 Z.-G. Gu, C.-H. Zhan, J. Zhang and X.-H. Bu, *Chem. Soc. Rev.*, 2016, **45**, 3122.
26 G.-J. Ren, Z. Chang, J. Xu, Z.-P. Hu, Y.-Q. Liu, Y.-L. Xu and X.-H. Bu, *Chem. Commun.*, 2016, **52**, 2079.
27 Y. Cui, B. Li, H. He, W. Zhou, B. Chen and G. Qian, *Acc. Chem. Res.*, 2016, **49**, 483.
28 Y.-S. Wei, M. Zhang, P.-Q. Liao, R.-B. Lin, T.-Y. Li, G. Shao, J.-P. Zhang and X.-M. Chen, *Nat. Commun.*, 2015, **6**, 8348.
29 H. Furukawa, K. E. Cordova, M. O'Keeffe and O. M. Yaghi, *Science*, 2013, **341**, 974.
30 Z. Li, N. M. Schweitzer, A. B. League, V. Bernales, A. W. Peters, A. Getsoian, T. C. Wang, J. T. Miller, A. Vjunov, J. L. Fulton, J. A. Lercher, C. J. Cramer, L. Gagliardi, J. T. Hupp and O. K. Farha, *J. Am. Chem. Soc.*, 2016, **138**, 1977.
31 C. He, K. Lu, D. Liu and W. Lin, *J. Am. Chem. Soc.*, 2014, **136**, 5181.
32 Y. Yue, J. A. Rabone, H. Liu, S. M. Mahurin, M.-R. Li, H. Wang, Z. Lu, B. Chen, J. Wang, Y. Fang and S. Dai, *J. Phys. Chem. C*, 2015, **119**, 9442.
33 H.-M. Wen, B. Li, H. Wang, C. Wu, K. Alfooty, R. Krishna and B. Chen, *Chem. Commun.*, 2015, **51**, 5610.
34 I. Spanopoulos, C. Tsangarakis, E. Klontzas, E. Tylianakis, G. Froudakis, K. Adil, Y. Belmabkhout, M. Eddaoudi and P. N. Trikalitis, *J. Am. Chem. Soc.*, 2016, **138**, 1568.
35 D.-X. Xue, Y. Belmabkhout, O. Shekhah, H. Jiang, K. Adil, A. J. Cairns and M. Eddaoudi, *J. Am. Chem. Soc.*, 2015, **137**, 5034.
36 T. M. McDonald, W. R. Lee, J. A. Mason, B. M. Wiers, C. S. Hong and J. R. Long, *J. Am. Chem. Soc.*, 2012, **134**, 7056.
37 N. C. Burtch, H. Jasuja and K. S. Walton, *Chem. Rev.*, 2014, **114**, 10575.
38 T. M. McDonald, D. M. D'Alessandro, R. Krishna and J. R. Long, *Chem. Sci.*, 2011, **2**, 2022.
39 Y. X. Ye, S. S. Xiong, X. N. Wu, L. Q. Zhang, Z. Y. Li, L. H. Wang, X. L. Ma, Q.-H. Chen, Z. J. Zhang and S. C. Xiang, *Inorg. Chem.*, 2016, **55**, 292.
40 D. S. Chen, H. Z. Xing, C. G. Wang and Z. M. Su, *J. Mater. Chem. A*, 2016, **4**, 2657.
41 J. A. Mason, T. M. McDonald, T.-H. Bae, J. E. Bachman, K. Sumida, J. J. Dutton, S. S. Kaye and J. R. Long, *J. Am. Chem. Soc.*, 2015, **137**, 4787.
42 P.-Q. Liao, X.-W. Chen, S.-Y. Liu, X.-Y. Li, Y.-T. Xu, M. N. Tang, Z. B. Rui, H. B. Ji, J.-P. Zhang and X.-M. Chen, *Chem. Sci.*, 2016, **7**, 6528.
43 G. Q. Kong, Z. D. Han, Y. B. He, S. Ou, W. Zhou, T. Yildirim, R. Krishna, C. Zou, B. L. Chen and C.-D. Wu, *Chemistry*, 2013, **19**, 14886.
44 L. Zhang, K. Jiang, M. Jiang, D. Yue, Y. Wan, H. Xing, Y. Yang, Y. Cui, B. Chen and G. Qian, *Chem. Commun.*, 2016, **52**, 13568.
45 K. Liu, D. Ma, B. Li, Y. Li, K. Yao, Z. Zhang, Y. Han and Z. Shi, *J. Mater. Chem. A*, 2014, **2**, 15823.
46 J. Jiao, H. Liu, F. Chen, D. Bai, S. Xiong and Y. He, *Inorg. Chem. Front.*, 2016, **3**, 1411.
47 Z.-J. Guo, J. Yu, Y.-Z. Zhang, J. Zhang, Y. Chen, Y. Wu, L.-H. Xie and J.-R. Li, *Inorg. Chem.*, 2017, **56**, 2188.
48 G. Chen, Z. Zhang, S. Xiang and B. Chen, *CrystEngComm*, 2013, **15**, 5232.
49 L. Zhang, C. Zou, M. Zhao, K. Jiang, R. Lin, Y. He, C.-D. Wu, Y. Cui, B. Chen and G. Qian, *Cryst. Growth Des.*, 2016, **16**, 7174.
50 H. Xu, Y. He, Z. Zhang, S. Xiang, J. Cai, Y. Cui, Y. Yang, G. Qian and B. Chen, *J. Mater. Chem. A*, 2013, **1**, 77.
51 X. Duan, Y. He, Y. Cui, Y. Yang, R. Krishna, B. Chen and G. Qian, *RSC Adv.*, 2014, **4**, 23058.